Moments of NMR Absorption Lines from the Free Induction decay or Echo in Solids

by Dianoux A.J., Sykora S., and Gutowsky H.S.

which appeared in

Journal of Chemical Physics, Volume 55, p 4768-4771 (1971)

Abstract

A new method is presented for determining the moments of nuclear magnetic resonance absorption lines from the shape of either the free induction decay or that of the echo. Unlike previously used techniques, this method does not require the assumption of an analytic function for the line shape or the fitting of the experimental decay with a polynomial. A fast, suitably precise and numerically stable algorithm has been developed for performing the integration required by the new method.

Keywords: NMR, Spectral moments, FID, Echo, Solid, Lineshape

Moments of NMR Absorption Lines from the Free Induction Decay or Echo of Solids*

A. J. DIANOUX, S. SÝKORA, AND H. S. GUTOWSKY
Department of Chemistry, University of Illinois, Urbana, Illinois 61801

(Received 20 May 1971)

A new method is presented for determining the moments of nuclear magnetic resonance absorption lines from the shape of either the free induction decay or that of the echo. Unlike previously used techniques, this method does not require the assumption of an analytic function for the line shape or the fitting of the experimental decay with a polynomial. A fast, suitably precise and numerically stable algorithm has been developed for performing the integration required by the new method.

The moments of the NMR absorption line of a solid are important structure-sensitive parameters. The increasing application of NMR rf-pulse methods to solids has led to an interest in determining the moments, especially the second moment, from the data obtained in such experiments. Two different approaches have been employed to extract the moments from the shape of either the free induction decay (FID) or that of the solid echo.

In one, the experimental decay curve is fitted by an assumed analytic function[1] and the moments are then calculated from the parameters describing the optimal fit. The main drawback of this method is the required assumption of a particular absorption line shape.

In the second approach, the beginning of the experimental decay curve is fitted by a polynomial.[2] The coefficient of t^{2n} in this expansion is then set equal to $(-1)^k M_{2k}/(2k!)$, where M_n denotes the nth moment. The odd moments are obtainable in the same way from the out-of-phase component of the induced signal. While avoiding any assumption about the line shape, this method is unreliable from a numerical point of view since, as we will describe in the discussion, very good fits may often be obtained with very different polynomials.

In this article we present a new method for determining the moments which requires neither an assumption about the functional form of the line shape nor the fitting of the experimental decay by an analytic function.

THEORETICAL

The nth moment of the absorption line $g(\omega)$ is defined as

$$M_n = \int_{-\infty}^{+\infty} \omega^n g(\omega_0+\omega)\,d\omega \Big/ \int_{-\infty}^{+\infty} g(\omega)\,d\omega, \qquad (1)$$

where ω_0 is the center of the band, chosen such that

$$M_1 = 0. \qquad (2)$$

The shape of the FID (or of the echo) obtained by phase-sensitive detection is

$$G(t,\alpha) = \mathrm{Re}\{\exp[i(\Omega t+\alpha)] \int_{-\infty}^{+\infty} g(\omega)\,\exp(-i\omega t)\,d\omega\}, \qquad (3)$$

where Ω is the irradiation frequency and α is the phase of the detector. If a pair of mutually orthogonal phase-sensitive detectors is used, for the first of which $\alpha \equiv \phi$, one obtains two FID curves described by

$$G_\phi(t) = G(t,\phi) = \mathrm{Re}\{\exp[i(\Omega t+\phi)] \int_{-\infty}^{+\infty} g(\omega) \times \exp(-i\omega t)\,d\omega\},$$

$$G_\phi'(t) = G(t,\phi+\tfrac{1}{2}\pi) = -\mathrm{Im}\{\exp[i(\Omega t+\phi)] \int_{-\infty}^{+\infty} g(\omega) \times \exp(-i\omega t)\,d\omega\}. \qquad (4)$$

The functions $G_\phi(t)$ and $G_\phi'(t)$ satisfy the relations,

$$G_\phi(-t) = G_\phi(t)\,\cos 2\phi - G_\phi'(t)\,\sin 2\phi,$$
$$G_\phi'(-t) = -G_\phi(t)\,\sin 2\phi - G_\phi'(t)\,\cos 2\phi. \qquad (5)$$

For $t=0$ these relations lead to the condition

$$\tan\phi = -G_\phi'(0)/G_\phi(0), \qquad (6)$$

which provides an operational definition of the phase ϕ. In particular, it makes it possible to adjust the phase-sensitive detector[3] until $G_\phi'(0)=0$ in which case $\phi=0$ [if $G_\phi(0)>0$].

Assuming that the phase has been properly adjusted, we introduce the notation

$$G_{\parallel}(t) = G(t,0) \quad \text{and} \quad G_\perp(t) = G(t,\tfrac{1}{2}\pi). \qquad (7)$$

Equation (5) now reduces to

$$G_{\parallel}(-t) = G_{\parallel}(t) \quad \text{and} \quad G_\perp(-t) = -G_\perp(t). \qquad (8)$$

From Eq. (4) it follows that:

$$g(\omega_0+\omega) = (2\pi)^{-1} \int_{-\infty}^{+\infty} [G_{\parallel}(t) - iG_\perp(t)] \times \exp[i(\omega-\delta)t]\,dt, \qquad (9)$$

where $\delta = \Omega - \omega_0$.

By substituting Eq. (9) in the definition of the first moment and using Eq. (8) to simplify the result, we obtain

$$M_1 = \delta + \dot{G}_\perp(0)/G_{\parallel}(0), \qquad (10)$$

where the dot denotes the derivative with respect to time. By Eq. (2), this implies that

$$\delta = \Omega - \omega_0 = -\dot{G}_\perp(0)/G_{\parallel}(0), \qquad (11)$$

which may serve as an operational definition of δ. Accordingly, to satisfy experimentally the on-resonance condition $\delta=0$, one simply adjusts ω_0 so that $\dot{G}_\perp(0)=0$, with $G_{||}(0)\neq 0$.

With this adjustment made, we may shift the origin of the frequency scale by putting $\omega_0=0$. Equation (9) then becomes

$$g(\omega)=(2\pi)^{-1}\int_{-\infty}^{+\infty}[G_{||}{}^r(t)-iG_\perp{}^r(t)]\exp(i\omega t)\,dt, \quad (12)$$

where the superscript r refers to the on-resonance condition. The even moments of $g(\omega)$ are identical with the corresponding moments of its symmetrical part which, by Eqs. (12) and (8), can be written as

$$g_s(\omega)=\pi^{-1}\,\mathrm{Re}\int_0^\infty G_{||}{}^r(t)\exp(i\omega t)\,dt. \quad (13)$$

Correspondingly, the odd moments of $g(\omega)$ are the moments of its antisymmetrical part

$$g_a(\omega)=\pi^{-1}\,\mathrm{Im}\int_0^\infty G_\perp{}^r(t)\exp(i\omega t)\,dt. \quad (14)$$

Note that $G_\perp{}^r(t)=0$ if the absorption line is symmetrical.

Next, we introduce quantities $Q_n(\epsilon)$ defined as

$$Q_n(\epsilon)=\int_{-\infty}^{+\infty}\frac{\omega^n}{1+(\epsilon\omega)^{1+n+\nu}}\,g(\omega)\,d\omega, \quad (15)$$

where ϵ is a positive parameter which has the dimension of time, and ν equals 1 for even n and 0 for odd n. The quantity $Q_n(\epsilon)$ is connected to the nth moment by the extrapolation formula

$$M_n=\lim_{\epsilon\to 0}Q_n(\epsilon)/G_{||}{}^r(0). \quad (16)$$

By using Eqs. (13)–(15) one may write

$$Q_{2n}(\epsilon)=\int_0^\infty G_{||}{}^r(t)f_{2n}(\epsilon,t)\,dt \quad (17a)$$

and

$$Q_{2n+1}(\epsilon)=\int_0^\infty G_\perp{}^r(t)f_{2n+1}(\epsilon,t)\,dt, \quad (17b)$$

in which the functions $f_n(\epsilon,t)$ are given as

$$f_{2n}(\epsilon,t)=\pi^{-1}\int_{-\infty}^{+\infty}\frac{\omega^{2n}}{1+(\epsilon\omega)^{2n+2}}\exp(i\omega t)\,d\omega, \quad (18a)$$

$$f_{2n+1}(\epsilon,t)=-\frac{i}{\pi}\int_{-\infty}^{+\infty}\frac{\omega^{2n+1}}{1+(\epsilon\omega)^{2n+2}}\exp(i\omega t)\,d\omega. \quad (18b)$$

For $\epsilon\neq 0$ these integrals converge and their values can be calculated directly from the residue theorem. The resulting formulas for the first several functions $f_n(\epsilon,t)$ are (for positive t):

$$f_1(\epsilon,t)=(1/\epsilon^2)\exp(-t/\epsilon),$$

$$f_2(\epsilon,t)=(1/\epsilon^3)\exp(-t/\sqrt{2}\epsilon)\cos[(t/\sqrt{2}\epsilon)+\tfrac{1}{4}\pi],$$

$$f_3(\epsilon,t)=(1/\epsilon^4)\exp(-t/\sqrt{2}\epsilon)\cos(t/\sqrt{2}\epsilon),$$

$$f_4(\epsilon,t)=(3\epsilon^5)^{-1}\{\exp(-t/\epsilon)+2\exp(-t/2\epsilon)\times\cos[(\sqrt{3}t/2\epsilon)+\tfrac{1}{3}\pi]\},$$

$$f_5(\epsilon,t)=(3\epsilon^6)^{-1}[\exp(-t/\epsilon)+2\exp(-t/2\epsilon)\times\cos(\sqrt{3}t/2\epsilon)]. \quad (19)$$

The individual moments can now be obtained from the observed decay functions $G_{||}{}^r(t)$ and $G_\perp{}^r(t)$ by combining Eqs. (16), (17), and (19). It is important to note that the limit, Eq. (16), is reached in each case with a zero slope since, from Eq. (15),

$$\lim_{\epsilon\to 0}dQ_n(\epsilon)/d\epsilon=0. \quad (20)$$

This greatly facilitates the extrapolation of $Q_n(\epsilon)$ for $\epsilon\to 0$.

The off-resonance condition of Eq. (11) may lead to experimental error when either the dead time or the experimental noise limits the data available in the vicinity of $t=0$. For this reason, we now consider the effects upon the moments of having $\delta\neq 0$. It may be shown that

$$\delta=\lim_{\epsilon\to 0}\int_0^{+\infty}G_\perp(t)f_1(\epsilon,t)\,dt/G_{||}(0). \quad (21)$$

Therefore, the extrapolation procedure used to determine the moments can serve also for an accurate determination of δ. By comparing Eq. (9) with Eq. (12) one obtains the relations,

$$G_{||}{}^r(t)=G_{||}(t)\cos(\delta t)-G_\perp(t)\sin(\delta t),$$
$$G_\perp{}^r(t)=G_\perp(t)\cos(\delta t)+G_{||}(t)\sin(\delta t), \quad (22)$$

which, once δ is known, enable one to calculate the moments from the off-resonance decays $G_{||}(t)$ and $G_\perp(t)$. Off-resonance measurements have lower sensitivity than on-resonance observations and there are additional experimental errors due to the oscillatory behavior of $G_{||}(t)$ and $G_\perp(t)$. Therefore, Eqs. (21) and (22) are best used to correct for small deviations from resonance.

COMMENTS ON THE NUMERICAL PROCEDURE

For $n\geq 2$ and for small ϵ, the functions $f_n(\epsilon,t)$ rapidly oscillate. This leads to substantial problems in the numerical integration required by Eq. (17). The simple Simpson rule proved, in fact, to be inadequate with any experimentally reasonable spacing between the digitized data. The choice of a smaller integration step, combined with suitable interpolation of the experimental data, increases the numerical stability but the calculation time increases as well. An algorithm

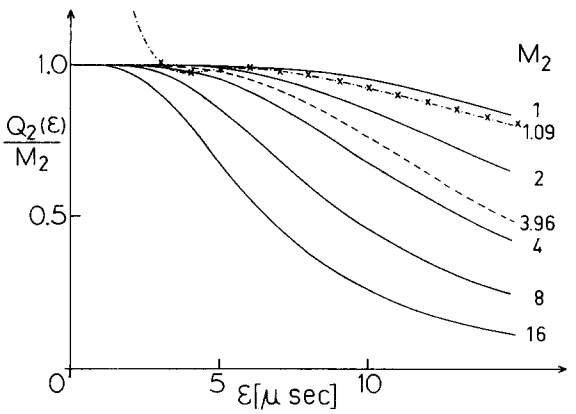

FIG. 1. Values of $Q_2(\epsilon)$ calculated numerically as a function of ϵ for several induction decay curves corresponding to different values of M_2 for fluorine nuclei. The solid lines are for "data" points generated with $G_{||}{}^r(t)=\exp(-\frac{1}{2}a^2t^2)$; the dashed line, with $G_{||}{}^r(t)=\exp(-\frac{1}{2}a^2t^2)\times(1/bt)\sin bt$. The points with dashed line are for the experimentally obtained $G_{||}{}^r(t)$ given in Fig. 2.

was developed which proved to be both fast and numerically stable.

A quadratic interpolation polynomial $y_i(t)=a_it^2+b_it+c_i$ is determined for each set of three consecutive experimental points $G(t_{i-1})$, $G(t_i)$, and $G(t_{i+1})$.[4] The contribution to $Q_n(\epsilon)$ arising from the interval $\tau_i\equiv\langle\frac{1}{2}(t_{i-1}+t_i),\frac{1}{2}(t_i+t_{i+1})\rangle$ is calculated as

$$q_n{}^i(\epsilon)=\int_{\tau_i}G(t)f_n(\epsilon,t)dt\cong\int_{\tau_i}y_i(t)f_n(\epsilon,t)dt, \quad (23)$$

using explicit formulas for the integral on the right-hand side of this equation. The quantity $Q_n(\epsilon)$ is then set equal to the sum of all $q_n{}^i(\epsilon)$ plus a similarly obtained correction term arising from the initial interval $\langle 0,\frac{1}{2}(t_1+t_2)\rangle$, where t_1 is the coordinate of the first experimental point.

At this point we have to stress that the difficulties connected both with the numerical stability and with the sensitivity of the results to experimental errors increase drastically with increasing order of the moment. We feel that with reasonably good experimental data it is possible to obtain at most reliable second and third moments and semiquantitative information about the fourth moment.

RESULTS AND DISCUSSION

In order to test the proposed method, we have performed the numerical integration required in Eq. (17a) for M_2, using for $G_{||}{}^r(t)$ analytically generated sets of "data" as well as experimentally obtained digitized data. Gaussian and more complicated decay curves[1] were generated with durations corresponding to second moments ranging from 1 to 16 G^2 for fluorine. The $G_{||}{}^r(t)$ values were calculated with a spacing of 1 μsec, which is experimentally feasible with a fast digitizer. In Fig. 1 we give the results obtained for the ratio $Q_2(\epsilon)/M_2$ as a function of ϵ for several of the generated decays.

The values obtained for the second and higher moments are very sensitive to the shape of the induction signal[4] $G(t)$ at small values of t. The quantity $Q_n(\epsilon)$ depends upon the full range of $G(t)$, but the weight given to $G(t)$ for large values of $|t|$ decreases rapidly with decreasing ϵ. This does not present any problem if the shape of $G(t)$ is known for all values of time, as in the case of echo experiments on solids—either the regular echo[2] or the recently reported "magic" echo.[5] However, the situation is substantially different for the free induction decay, for which data are not obtainable during the dead time $\langle 0, t_d\rangle$ following the rf pulse.

The latter point is shown in Fig. 2 which reproduces the experimental, time-averaged FID of the fluorine NMR in solid $KAsF_6$ powder at room temperature, observed with a pulse spectrometer operating at 25 MHz. The data are digitized for every microsecond, and the dead time is about 12 μsec. This dead time leads to the drastic divergence in the values obtained for $Q_2(\epsilon)$ at small values of ϵ, illustrated in Fig. 1 by the numerical results corresponding to the experimental FID in Fig. 2. If the divergence occurs before $Q_2(\epsilon)$ has approached M_2 to a suitable degree of accuracy, the data are inadequate for the determination. It may be shown that the fault lies in the lack of data and not in the mathematical procedure employed.

On physical grounds, one would expect the divergence to occur when $\epsilon\lesssim t_d$, which is verified by our numerical results, those in Fig. 1 for $KAsF_6$ being typical. It is seen that $Q_2(\epsilon)$ diverges for $\epsilon<6$ μsec, with t_d about 12 μsec. Moreover, a smaller value of ϵ is required for $Q_2(\epsilon)$ to approach a larger value of M_2. This enables limits to be placed upon t_d for establishing M_2 to a given accuracy. Our results in Fig. 1 indicate that if an

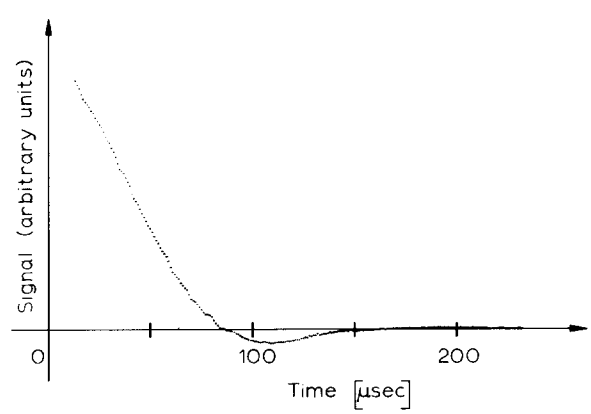

FIG. 2. The time-averaged ^{19}F free induction decay observed at 25 MHz for $KAsF_6$ powder at room temperature. The data are digitized at 1-μsec intervals following a dead time of about 12 μsec. Only the in-phase component $G_{||}{}^r(t)$ of the induction signal was observed.

accuracy of better than 5% is desired in M_2, the dead time must meet the condition

$$t_d \lesssim 2.5\times 10^5/(M_2)^{1/2}, \tag{24}$$

where t_d is in microseconds and M_2 is in square radians per square second.

The dead-time problem can be approached or avoided in several other ways. One can attempt to correct the beginning of the decay curve for the distortion due to slow recovery of the receiver from saturation. A method has been described by Barnaal and Lowe[6] for this purpose. Also, Jeener and Broekaert[7] have developed an experimental technique which enables one in principle to measure $G(t)$ for small value of t, but the procedure is laborious. The best pulse method for determining the shape of $G(t)$ seems to be the "magic" echo,[5] since it is practically free of the nonlinear attenuation effects unavoidable[2] in the case of the regular echo.

The estimation of M_2 by the numerical procedure outlines in connection with Eq. (17a) does appear to have practical advantages over the fitting of an induction decay with a series expansion and calculating M_2 from the coefficient of the t^2 term.[2] Data limited by receiver recovery time may be fitted by a polynomial which in turn gives what appears to be a mathematicaly definite M_2, but which may actually be erroneous. In contrast, as shown by the curves in Fig. 1 for the FID of Fig. 2, our method of calculation leads to visible divergences when the values calculated for the moments become physically unreliable.

A comparative study was made of the propagation of errors in the two methods, with the results summarized in Table I. A "set of data" was generated for $G_{||}{}'(t)$ by means of a Gaussian decay, corresponding to a second moment of 8 G^2 for fluorine, digitized at intervals of 1 μsec with an rms noise amplitude taken to be 1% of $G(0)$. These "data" were then employed with and without the noise to calculate M_2 by the two methods. The percent difference Δ_0 between the actual M_2 and the apparent value determined from the "data" without noise measures the error introduced by the approximation method itself. In turn, the percent spread $\pm\Delta$ in the apparent M_2 produced by the noise is a measure of how sensitive the method is to error propagation.

In the polynomial method, the "data" were fitted by polynomials ranging from the second to the eighth degree, in order to assess the improvement in accuracy of the calculated M_2 with the improvement in fit of the "data" by using higher powers in the expansion. Inasmuch as the polynomial is usually fitted to the beginning portion of the decay, we tried fitting the "data" over three different regions, from $t=0$ to the t's at which

TABLE I. A comparison of the polynomial fitting method with that proposed herein for determining M_2 from an induction decay. Both methods were applied to a generated set of "data" points from a Gaussian decay at intervals of 1 μsec with an rms noise amplitude of 1% of $G(0)$. The errors Δ_0 and $\pm\Delta$ are given in percent, with $\Delta_0 \equiv (M_2,\text{actual}-M_2,\text{apparent})/(M_2,\text{actual})$ and $\pm\Delta$ describing the range in M_2,apparent produced by the noise.

	Region A $G(0)$ to $\frac{3}{4}G(0)$		Region B $G(0)$ to $\frac{1}{2}G(0)$		Region C $G(0)$ to $\frac{1}{10}G(0)$	
Method[a]	Δ_0	$\pm\Delta$	Δ_0	$\pm\Delta$	Δ_0	$\pm\Delta$
$n=2$	12.5	12	24	6	54	4
$n=4$	1.5	33	2.5	14	19	7
$n=6$	0.2	51	0.6	32	5	11
$n=8$	0.04	90	0.1	50	1	22
Eq. (17a)	not applicable		not applicable		0	6

[a] The values listed for n describe the degree of the polynomial employed in fitting the induction decay "data."

$G(t)$ had fallen to $\frac{3}{4}$, $\frac{1}{2}$, and $\frac{1}{10}$ of its initial value, $G(0)$. The results in Table I exhibit several trends. For a polynomial of given degree, using less of the decay gives an apparent value of M_2 which is likely to be closer to the theoretical value but which is more sensitive to the experimental noise. A similar trend is found as one increases the degree of the fitted polynomial for a given portion of the induction decay. Also, it is clear that even with very good experimental data, e.g., the assumed rms noise level of 1% of $G(0)$, the polynomial method is not well suited for determining values of M_2 because it does not minimize both systematic and probable errors. In contrast, with the same data, our method proves to be substantially more reliable. Moreover, if the data do not contain sufficient information to determine M_2, either because of the dead time as mentioned above, or because of an inadequate signal-to-noise ratio, the function $Q_2(\epsilon)$ either diverges or oscillates for small ϵ and its extrapolation for $\epsilon\to 0$ is therefore impossible.

* This research was supported by the National Science Foundation and by the U.S. Office of Naval Research.

[1] A. Abragam, *The Principles of Nuclear Magnetism* (Clarendon, Oxford, England, 1961), pp. 114ff.

[2] J. G. Powles and J. H. Strange, Proc. Phys. Soc. (London) **82**, 6 (1963).

[3] This adjustment can be made more precisely somewhat off resonance because then the derivative of $G'(t)$ at $t=0$ is nonzero; see Eq. (11).

[4] When it cannot lead to any mistake, the indices are omitted.

[5] W.-K. Rhim, A. Pines, and J. S. Waugh, Phys. Rev. Letters **25**, 218 (1970); Phys. Rev. B **3**, 684 (1971).

[6] D. E. Barnaal and I. J. Lowe, Rev. Sci. Instr. **37**, 428 (1966).

[7] J. Jeener and P. Broekaert, Phys. Rev. **157**, 232 (1967).